Environmental Pollution xxx (xxxx) xxx

Contents lists available at ScienceDirect

Environmental Pollution

journal homepage: www.elsevier.com/locate/envpol

Corrigendum to ‘Machine-learning-based corrections of CMIP6 historical surface ozone in China during 1950–2014’ [Environ. Pollut. **357** (2024) 124397]

Yuanxi Tong [a], Yingying Yan [a,*], Jintai Lin [b], Shaofei Kong [a,c], Zhixuan Tong [a], Yifei Zhu [a], Yukun Yan [a], Zhan Sun [a]

[a] *Department of Atmospheric Science, School of Environmental Sciences, China University of Geosciences, Wuhan, 430074, China*
[b] *Laboratory for Climate and Ocean-Atmosphere Studies, Department of Atmospheric and Oceanic Sciences, School of Physics, Peking University, Beijing, 100871, China*
[c] *Research Centre for Complex Air Pollution of Hubei Province, Wuhan, 430074, China*

The authors regret When the concentration unit of surface ozone is converted from μg m^{-3} to ppb, the formula ppb= (Molecular weight/ Molar volume of gas) μg m^{-3} is incorrectly written as μg m^{-3}= (Molecular weight/Molar volume of gas) ppb. Related content errors occur. After the correct unit conversion formula is applied, Figs. 2, 3, 4, 5, 6, 8 and Fig S3 should be replaced with the corresponding text content.

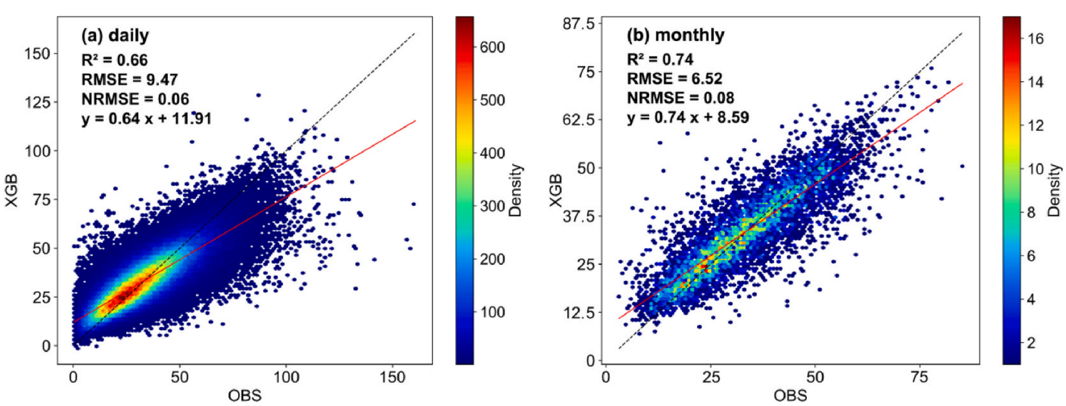

Fig. 2 Daily (a) and monthly (b) scatter density plot of the cross-validation result for the final estimator.

Replace the corresponding text with: On average, for daily retrievals, the XGB model shows a reliable overall accuracy, with a high cross-validated coefficients of determination (R^2 = 0.66), a corresponding root-mean-square error (RMSE) of 9.47 ppb, and normalized root-mean-square error (NRMSE) of 0.06. The minor difference in the statistical meterics between the day and month (R^2 = 0.74; RMSE = 6.52 ppb, NRMSE = 0.08) level indicates that averaging over time reduces the errors and there is no obvious temporal overfitting in this model.

DOI of original article: https://doi.org/10.1016/j.envpol.2024.124397.
* Corresponding author.
E-mail address: yanyingying@cug.edu.cn (Y. Yan).

https://doi.org/10.1016/j.envpol.2024.125004

0269-7491/© 2024 Elsevier Ltd. All rights are reserved, including those for text and data mining, AI training, and similar technologies.

Please cite this article as: Yuanxi Tong et al., *Environmental Pollution,* https://doi.org/10.1016/j.envpol.2024.125004

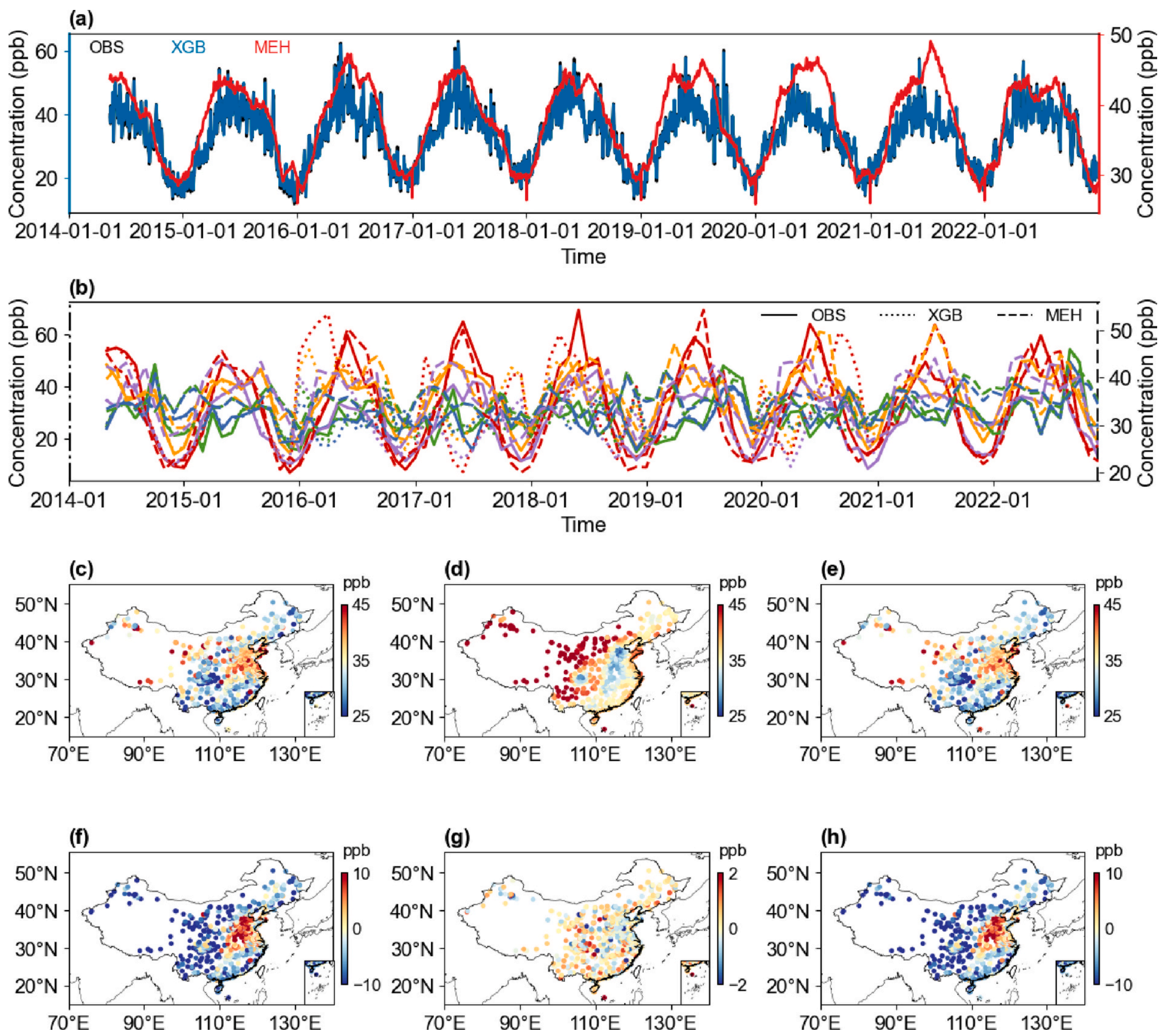
(a)
OBS
XGB
MEH
Concentration (ppb)
Time
(b)
OBS
XGB
MEH
Concentration (ppb)
Time
(c)
(d)
(e)
(f)
(g)
(h)
ppb

Fig. 3 The time series of daily mean ozone concentrations averaged over China (a) and monthly mean ozone averaged over five key focus regions (b) for OBS, MEH and XGB from 2014 to 2022. The ozone spatial distribution for OBS (c), MEH (d) and XGB (e) averaged over this period. Also shown are the differences between OBS and MEH (f), between XGB and OBS (g), between XGB and MEH (h).

Replace the corresponding text with: Spatially, average ozone mixing raitos for the years 2014–2022 show roughly opposite spatial patterns, as shown in Fig. 3c, d and 3f. Such deviations are effectively alleviated by the XGB model, with the biases declined to be −2.28–2.34 ppb (−6.87%–7.05%).

(0.21–0.88 ppb yr^{-1}) (Yeo and Kim, 2021), in the North China Plain (1.58 ppb yr^{-1} from 2006 to 2017) and eastern China (2.3 ppb yr^{-1} from 2013 to 2017) (Cheng et al., 2019; Li et al., 2019). Through an extensive literature review, Sicard (2021) has concluded that ozone concentrations increased in most regions of East Asia with an enhancement of 0.21 ppb yr^{-1} at rural stations over the period 2000–2010 and 0.68 ppb yr^{-1} in cities between 2015 and 2014. However, the upward trends simulated by MEH are 0.17 ppb yr^{-1} (China), 0.10 ppb yr^{-1} (BTH), 0.15 ppb yr^{-1} (YRD), 0.22 ppb yr^{-1} (PRD), 0.14 ppb yr^{-1} (MYR) and 0.14 ppb yr^{-1} (CC), respectively. This indicates that the MEH model also misestimates the long-term trend of ozone concentration.

The XGB ozone results show that daily mean ozone concentration

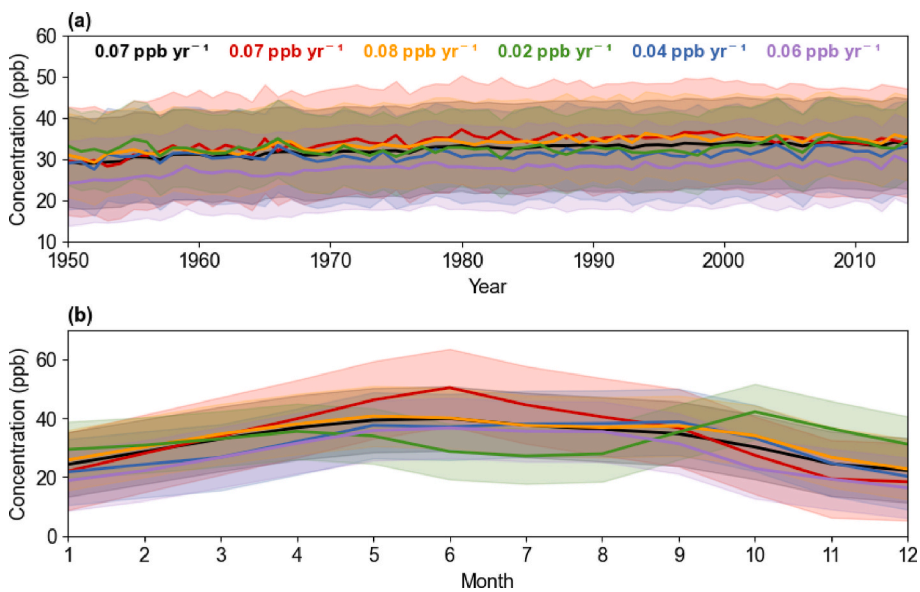

Fig. 4 The average annual (a) and monthly (b) ozone concentrations over China, BTH, YRD, PRD, MYR, CC simulated by XGBoost from 1950 to 2014, the shadow represents the standard deviation and the numbers represent the long-term trends.

Replace the corresponding text with: During the period 1950–2014, ozone concentrations show an increasing trend (Fig. 4a). The average enhancements are 0.07 ppb yr^{-1} for China, 0.07 ppb yr^{-1} for BTH, 0.08 ppb yr^{-1} for YRD, 0.02 ppb yr^{-1} for PRD, 0.04 ppb yr^{-1} for MYR, and 0.06 ppb yr^{-1} for CC, respectively. Due to the long time horizon of this study, the growth trends are lower than those reported in other studies after smoothing effect, such as 0.28–1.02 ppb yr^{-1} in the PRD from 2006 to 2019 (Li et al., 2022), 0.58 ppb yr^{-1} in Hong Kong, China from 1994 to 2007 (Wang et al., 2009), and 0.51 ppb yr^{-1} in Taiwan, China from 1994 to 2012 (Chen et al., 2014). They are also lower than the ozone trends observed in Japan from 1980 to 2005 (0.27 ppb yr^{-1}) (Nagashima et al., 2017), in some areas of South Korea from 2001 to 2018 without climate change effects is estimated to be 30 ppb in the year 1950 averaged over China (Fig. 4). This result is consistent with the baseline ozone concentrations of North America (<60 ppb, Emery et al., 2012), Europe (<50 ppb, Derwent et al., 2018), and East Asia (<80 ppb, Lam and Cheung, 2022). It indicates that the increase in anthropogenic emissions of China has a significant contribution to ozone enhancement between 1950 and 2014.

In addition, significant differences in the seasonal variations of ozone concentration exist due to latitude. For example, compared with the PRD, BTH is located at a higher latitude, showing a more significant change (up to 32 ppb; Fig. 4b) in ozone concentration due to the notable seasonal changes in temperature, solar radiation, and other meteorological factors. Conversely, the PRD, located at a lower latitude, shows a moderate seasonal variations (∼15 ppb) in ozone concentration due to relatively stable temperature and solar radiation throughout the year.

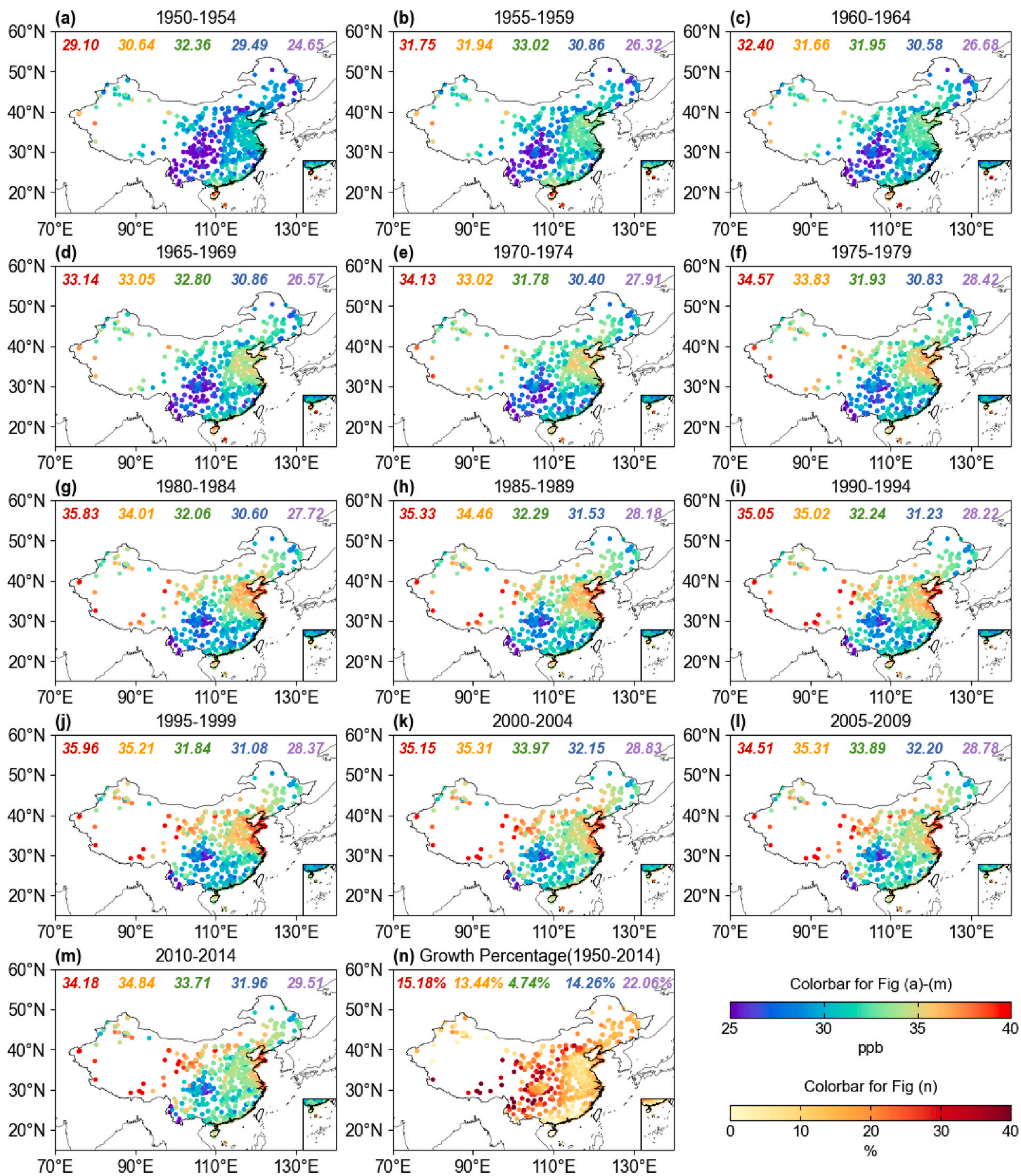
(a) 1950-1954
29.10 30.64 32.36 29.49 24.65
(b) 1955-1959
31.75 31.94 33.02 30.86 26.32
(c) 1960-1964
32.40 31.66 31.95 30.58 26.68
(d) 1965-1969
33.14 33.05 32.80 30.86 26.57
(e) 1970-1974
34.13 33.02 31.78 30.40 27.91
(f) 1975-1979
34.57 33.83 31.93 30.83 28.42
(g) 1980-1984
35.83 34.01 32.06 30.60 27.72
(h) 1985-1989
35.33 34.46 32.29 31.53 28.18
(i) 1990-1994
35.05 35.02 32.24 31.23 28.22
(j) 1995-1999
35.96 35.21 31.84 31.08 28.37
(k) 2000-2004
35.15 35.31 33.97 32.15 28.83
(l) 2005-2009
34.51 35.31 33.89 32.20 28.78
(m) 2010-2014
34.18 34.84 33.71 31.96 29.51
(n) Growth Percentage(1950-2014)
15.18% 13.44% 4.74% 14.26% 22.06%
60°N
50°N
40°N
30°N
20°N
70°E
90°E
110°E
130°E
Colorbar for Fig (a)-(m)
25
30
35
40
ppb
Colorbar for Fig (n)
0
10
20
30
40
%

Fig. 5 The spatial distribution of the average ozone concentration of XGB retrievals in every five years from 1950 to 2014 (a–m), and the spatial distribution of ozone growth percentage from 1950 to 2014 (n), with the numbers represent the corresponding values of BTH, YRD, PRD, MYR, and CC regions.

Replace the corresponding text with: The ozone concentration in the CC has been relatively low with an annual mean value from 25 ppb (1950–1954) to 30 ppb (2010–2014), but has increased most significantly during this period with a growth rate of 22.06% (Fig. 5n). In the regions of BTH, YRD, and the areas between them, ozone concentration increased from 1950 (BTH: 29 ppb; YRD: 31 ppb) to 1999 (BTH: 36 ppb; YRD: 35 ppb), then slightly decreased from 2000 to 2014 (BTH: 34 ppb; YRD: 35 ppb).

The ozone of MYR also experiences similar changes, but the upward and trends of ozone for the period 1950–2009 (30 ppb versus 32 ppb) are moderate, and the decline from 2010 to 2014 is less obvious.

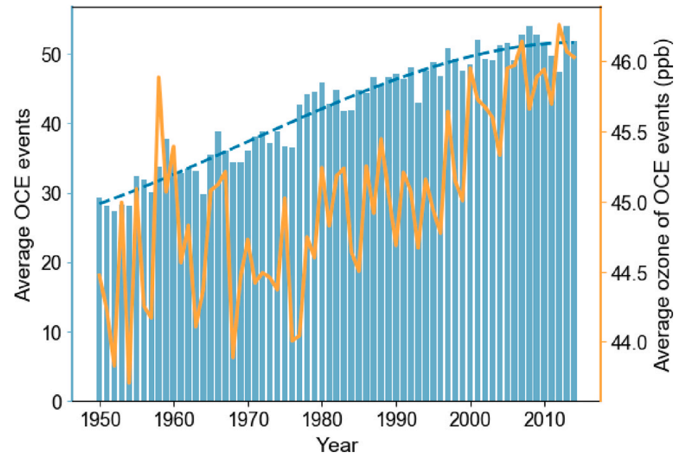

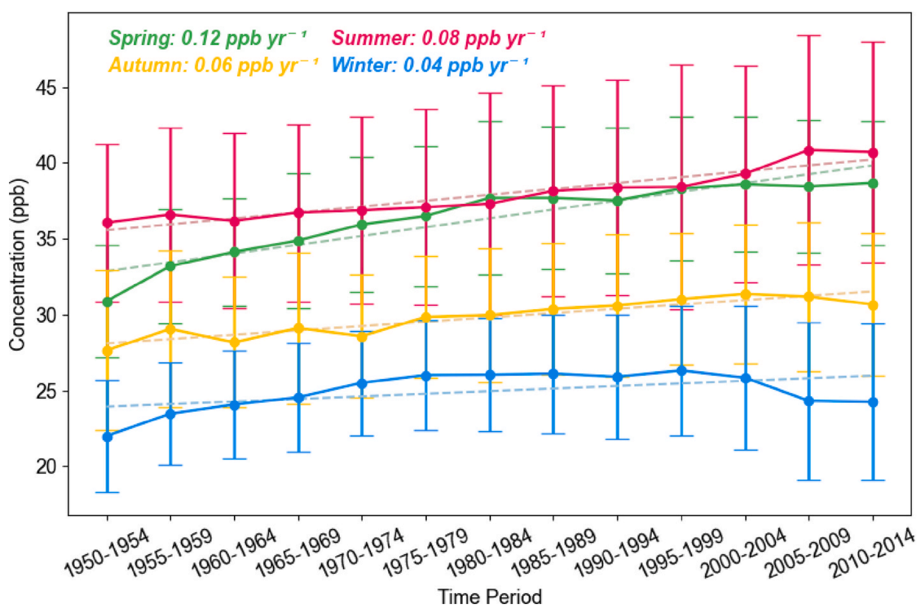

Fig. 6 Seasonal surface ozone concentration averaged over every five years from 1950 to 2014 (spring for MAM, summer for JJA, autumn for SON, winter for DJF) after bias–corrected by XGBoost, the bar represents standard error and the fitting line represents the long-term trend.

Replace the corresponding text with: The seasonal variations are depicted in Fig. 6. During the period of 1950–2014, the ozone concentration increases at rates of 0.12 ppb yr^{-1}, 0.08 ppb yr^{-1}, 0.06 ppb yr^{-1}, and 0.04 ppb yr^{-1} in spring, summer, autumn, and winter, respectively.

Fig. 8 The number of OCE events (blue bar) with ozone concentration exceeding the standard (daily mean ozone≥70 μg m^{-3}) per year averaged over all stations from 1950 to 2014 after bias–corrected by XGBoost. The average ozone concentration of OCE events in each year (orange line). The blue dashed line is the fitting line of OCE events.

Replace the corresponding text with: The annual mean ozone averaged over OCE events also shows a fluctuating upward pattern, with the highest value of 46.27 ppb in 2012.

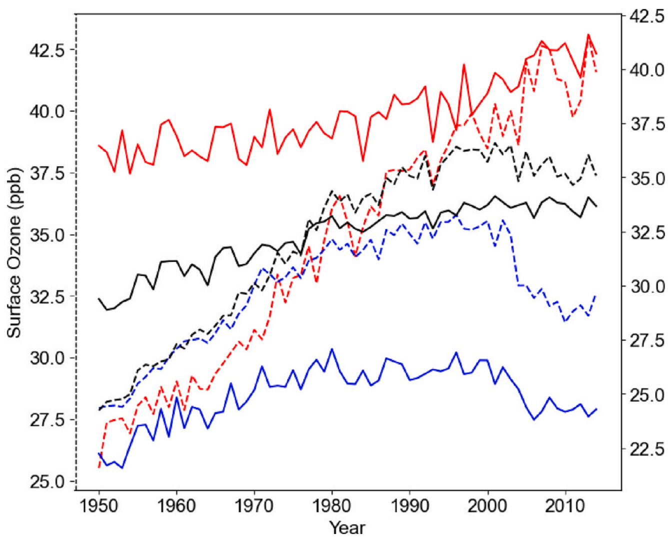

Fig. S3 Annual variation for MEH and XGB ozone concentration. The dashed line represents MEH, the full line represents XGB. Black, red and blue represents annual, summer and winter respectively.

Replace the corresponding text with: The XGB-derived ozone show a total ozone growth of 4.3 ppb, while the MEH-simulated ozone reproduce an increase of 9.52 ppb between 1950 and 2014.

In abstract, replace the corresponding text with:

The results reveal that CMIP6 historical simulations have a large deviation in ozone concentrations and their trends.

The daily mean ozone concentration without climate change effects is estimated to be 30 ppb in the year 1950 averaged over China.

In conclusions, replace the corresponding text with:

The MEH model severely misestimates the surface ozone concentrations, with approximately 55.3% of stations showing an error of more than ±5 ppb. Using the XGBoost algorithm for inversion or extrapolation is reasonable, with R^2 value of 0.66 and 0.74 for daily and monthly retrievals, respectively. Based on the XGB-derived surface ozone, concentrations in most parts of China have shown an increasing trend from 1950 to 2014, with growth rates ranging from 0.02 ppb yr^{-1} to 0.08 ppb yr^{-1}. The most significant increment in ozone is estimated in the CC region. Seasonally, the ozone enhancement is largest in spring and smallest in winter, with increasing trends ranging from 0.04 ppb yr^{-1} to 0.12 ppb yr^{-1}. The frequency and concentration of OCE events have increased significantly over time. During the period from 1950 to 1954 and 2010 to 2014, OCE events increased by 76.89%, with a concentration increase of 1.56 ppb.

The authors would like to apologise for any inconvenience caused.

References

Chen, S., Chang, C., Liu, J., Chou, C.C.-., Chang, J.S., Wang, J., 2014. Recent improvement in air quality as evidenced by the island-wide monitoring network in Taiwan. Atmos. Environ. 96, 70–77. https://doi.org/10.1016/j.atmosenv.2014.06.060.

Cheng, N., Li, R., Xu, C., Chen, Z., Chen, D., Meng, F., Cheng, B., Ma, Z., Zhuang, Y., He, B., 2019. Ground ozone variations at an urban and a rural station in Beijing from 2006 to 2017: trend, meteorological influences and formation regimes. J. Clean. Prod. 235, 11–20. https://doi.org/10.1016/j.jclepro.2019.06.204.

Derwent, R.G., Manning, A.J., Simmonds, P.G., Gerard spain, T., O'doherty, S., 2018. Long-term trends in ozone in baseline and European regionally-polluted air at Mace Head, Ireland over a 30-year period. Atmos. Environ. 179, 279–287. https://doi.org/10.1016/j.atmosenv.2018.02.024.

Emery, C., Jung, J., Downey, N., Johnson, J., Jimenez, M., Yarwood, G., Morris, R., 2012. Regional and global modeling estimates of policy relevant background ozone over the United States. Atmos. Environ. 47, 206–217. https://doi.org/10.1016/j.atmosenv.2011.11.012.

Lam, Y.F., Cheung, H.M., 2022. Investigation of policy relevant background (PRB) ozone in East Asia. Atmosphere 13 (5), 723. https://doi.org/10.3390/atmos13050723.

Li, K., Jacob, D.J., Liao, H., Shen, L., Zhang, Q., Bates, K.H., 2019. Anthropogenic drivers of 2013–2017 trends in summer surface ozone in China. Proc. Natl. Acad. Sci. USA 116 (2), 422–427. https://doi.org/10.1073/pnas.1812168116.

Li, X., Yuan, B., Parrish, D.D., Chen, D., Song, Y., Yang, S., Liu, Z., Shao, M., 2022. Long term trend of ozone in southern China reveals future mitigation strategy for air pollution. Atmos. Environ. 269, 118869. https://doi.org/10.1016/j.atmosenv.2021.118869.

Nagashima, T., Sudo, K., Akimoto, H., Kurokawa, J., Ohara, T., 2017. Long-term change in the source contribution to surface ozone over Japan. Atmos. Chem. Phys. 17 (13), 8231–8246. https://doi.org/10.5194/acp-17-8231-2017.

Sicard, P., 2021. Ground-level ozone over time. An observation-based global overview 19, 100226. https://doi.org/10.1016/j.coesh.2020.100226.

Wang, T., Wei, X.L., Ding, A.J., Poon, C.N., Lam, K.S., Li, Y.S., Chan, L.Y., Anson, M., 2009. Increasing surface ozone concentrations in the background atmosphere of Southern China, 1994–2007. Atmos. Chem. Phys. 9 (16), 6217–6227. https://doi.org/10.5194/acp-9-6217-2009.

Yeo, M.J., Kim, Y.P., 2021. Long-term trends of surface ozone in Korea. J. Clean. Prod. 294, 125352. https://doi.org/10.1016/j.jclepro.2020.125352.